Published paper:

D. Žarko and S. Stipetić, "Criteria for optimal design of interior permanent magnet motor series," *Electrical Machines (ICEM), 2012 XXth International Conference on*, Marseille, 2012, pp. 1242-1249.

http://dx.doi.org/10.1109/ICElMach.2012.6350035

Criteria for Optimal Design of Interior Permanent Magnet Motor Series

Damir Žarko, Stjepan Stipetić

Abstract—**This paper presents a general approach to the optimized design of a series of interior permanent magnet motors with the same lamination cross section. A concept of a referent and particular design has been introduced and analytical expressions which relate the principal machine parameters for the referent and particular machine have been derived. The referent design can be optimized according to a certain criterion which automatically yields the optimal design of the entire series. The particular designs are then obtained from the referent design by varying the stack length, the number of turns per coil and the number of parallel circuits. In order to demonstrate the correctness of the derived design principles the optimized design of a referent machine with IEC frame size 160 has been made by combining the finite-element method and Differential Evolution optimization algorithm from which five particular designs with power ratings ranging from 15 kW to 110 kW have been derived.**

Index Terms—**Electric machines, flux-weakening operation, interior permanent magnet machines, optimization, series of machines**

I. Introduction

Designers of electrical machines often use a single design of stator and rotor laminations for a set or series of machines designed for various power ratings at equal rated speed. For each machine in the series the stack length, number of turns per coil and number of parallel circuits are chosen for a particular power rating. The main reason for this approach is to reduce the cost of the tools for punching laminations of all the machines in a series, but also to fit the machines into the frame with standard size and shaft height.

The main issue is how to obtain the lamination cross-section which will be equally suitable for all particular designs in the series. In the case of interior permanent-magnet (IPM) machines it is important to yield rated torque at the same speed and constant power up to the same maximum speed for all designs. In this particular case it is also assumed that the maximum available voltage from the power converter is the same for the entire series, although the voltage may also vary. The basic idea is to define a "referent" machine design with carefully chosen stack length, one turn per coil and one parallel circuit as a base for the series. If the referent design is optimized in some sense, so will be the entire series sharing the same lamination geometry.

All the key parameters for a particular machine with specified power rating can be related to the calculated parameters of already optimized referent machine by using simple equations. It can be easily shown that the developed electromagnetic torque is proportional only to the stack length if the single lamination design is used, while some other parameters, e.g. inductances and resistances, have components related to the end region as well. The end-winding inductance or resistance changes with the number of turns per coil or number of parallel circuits, but the length of the end-winding remains the same for a specific lamination design irrespective of the chosen stack length. This leads to some nonlinear relationships between certain design parameters for the referent and particular design (saliency ratio, characteristic current, efficiency, power factor).

A problem of an optimal design of the series or sets of machines was not thoroughly addressed throughout the literature. Alberti *et.al.* [1] used combined finite-element and analytical analysis to design a lamination for a set of induction motors for the elevator systems. Similar to this paper, their approach involves a normalized motor design with unit stack length (1 meter) and one conductor per slot which is then scaled to various voltage and power ratings. The formal mathematical optimization of the normalized motor was not conducted.

The IPM motor structure which has been used in this paper is a slightly modified version of the integrated starter-alternator with two layers of cavities designed by Lovelace *et.al.*, [2], [3] [4]. Those authors also developed an optimized design of the motor based on the lumped parameter model and Monte Carlo optimization method. In order to minimize the torque ripple, flux barriers can be selected according to [5].

The initial optimization goal in this paper is to maximize the torque density, but also to ensure the constant power operation up to desired maximum speed. The universal approach to ensure maximum extension of the constant power region would be to aim for the satisfaction of the criterion for optimal field weakening first shown by Schiferl and Lipo [6]. This criterion makes the magnet flux linkage equal to the maximum direct axis stator flux linkage and therefore insures theoretically constant power operation up to infinite speed.

This paper demonstrates a general approach to design of an IPM motor series involving finite-element method (FEM) and Differential Evolution (DE) optimization algorithm. On an example of five particular designs in the series derived from the optimized referent design it is shown that it is possible to tune all the particular designs very close to the desired power ratings and close to the desired corner speed while ensuring the extension of the constant power region up to the targeted maximum speed. The perfect tuning is not always possible due to discrete ratios of the number of turns per coil and the number of parallel circuits.

II. Equations

The basic flux linkage, voltage and torque equations of an IPM motor with cross saturation effect included are given

D. Žarko and S. Stipetić are with the University of Zagreb, Faculty of Electrical Engineering and Computing, Department of Electrical Machines, Drives and Automation, Unska 3, HR-10000 Zagreb, Croatia (e-mail: dzarko@esa.fer.hr, sstipetic@esa.fer.hr)

as follows:

$$V = \sqrt{V_q^2 + V_d^2} \tag{1}$$
$$V_q = R_a I_q + \omega \Psi_d \tag{2}$$
$$V_d = R_a I_d - \omega \Psi_q \tag{3}$$
$$\Psi_d = \Psi_{md} + L_d I_d + L_{dq} I_q \tag{4}$$
$$\Psi_q = \Psi_{mq} + L_q I_q + L_{qd} I_d \tag{5}$$
$$V_q = R_a I_q + \underbrace{\omega \Psi_{md}}_{E_q} + \underbrace{\omega L_d}_{X_d} I_d + \underbrace{\omega L_{dq}}_{X_{dq}} I_q \tag{6}$$
$$V_d = R_a I_d - \underbrace{\omega \Psi_{mq}}_{E_d} - \underbrace{\omega L_q}_{X_q} I_q - \underbrace{\omega L_{qd}}_{X_{qd}} I_d \tag{7}$$
$$T_{em} = \frac{3}{2} p \Big[\Psi_{md} I_q - \Psi_{mq} I_d + (L_d - L_q) I_d I_q + L_{dq} I_q^2 - L_{qd} I_d^2 \Big] \tag{8}$$

where V_d, V_q, Ψ_d, Ψ_q, Ψ_{md}, Ψ_{mq}, I_d, I_q, L_d, L_q, E_d, E_q are the direct and quadrature axis components of the armature winding voltage, total flux linkage, flux linkage due to permanent magnet flux, current, inductance and back-emf respectively, R_a is the armature winding resistance, L_{dq} and L_{qd} are the cross-saturation inductances, and p is the number of pole pairs.

In the following discussion the terms with subscript 0 are used for parameters and expressions related to a *referent* machine design with preset stack length (l_{stk0}), one turn per coil ($N_c = 1$) and all turns per phase connected in series ($a_p = 1$). A machine design from the series with the same lamination cross-section as the referent design will be referred to as a *particular* machine design and, in general, will have different power rating, stack length l_{stk}, number of turns per coil N_c and number of parallel circuits a_p than the referent design. The purpose of the referent design, as will be shown later in the paper, is to define the lamination cross-section which can be optimized according to some criterion, e.g. maximum torque density, maximum efficiency, flux weakening performance etc., and prove that this optimization criterion is satisfied for all particular designs in the series with different stack length and the same lamination cross-section as the referent design.

The stack length of the referent machine can be chosen arbitrarily if the end-winding resistance and inductances can be neglected. In reality this is often not the case, especially for short lamination stacks, in which case it is advisable to set l_{stk0} to a value for which the variation of crucial parameters of the particular designs in the series, e.g. normalized characteristic current, will be minimal compared to the optimized referent design.

For the particular designs in the series the following general assumptions are made:

- All designs have the same lamination cross-section as the referent design,
- The rated (corner) speed of all designs at which the maximum available voltage from the power converter is utilized and above which the flux weakening regime starts should be the same as the rated speed of the referent design,
- The maximum available DC bus voltage for all particular designs is the same. The number of turns per coil and the number of parallel circuits for each design are determined based on its stack length and the available DC bus voltage,
- The maximum speed at which constant power is still attained is the same for all designs,
- All designs have the same current density and hence the same total ampere-turns and linear current density as the referent design.

The rated terminal current of a referent machine design with two-layer winding is given as

$$I_0 = \frac{1}{2} J A_{slot} f_{fill} \tag{9}$$

where J is the current density, A_{slot} is the total area of the slot and f_{fill} is the slot fill factor (typically around 0.4 for varnish insulated copper wire). The factor of $1/2$ is introduced due to two-layer winding. The current is generally consisted of direct (I_{d0}) and quadrature component (I_{q0}) where

$$I_0 = \sqrt{I_{d0}^2 + I_{q0}^2}. \tag{10}$$

In the general case of a machine with N_c turns per coil and a_p parallel circuits the line current I is equal to

$$I = \sqrt{I_d^2 + I_q^2} = \sqrt{\left(\frac{a_p}{N_c} I_{d0}\right)^2 + \left(\frac{a_p}{N_c} I_{q0}\right)^2} = \frac{a_p}{N_c} I_0 \tag{11}$$

The flux linkages, inductances and winding resistances have components related to the active machine part (core) and to the end-winding region (subscript co used further in the paper denotes component related to the core region and subscript ew denotes component related to the end-winding region). The end-winding arrangement and the average length of the end-coil is specific for a given lamination design regardless of the actual stack length, but a particular machine will in general have different N_c and a_p than the referent machine and hence its end-winding parameters will differ. The end-winding components of flux linkages and the corresponding inductances are equal in both direct and quadrature axis. Since there is no cross-saturation effect in the end region, the cross-saturation inductances refer only to the core region.

The direct and quadrature components of flux linkages and inductances for the referent machine with distinction of the core and end-winding region can be written as

$$L_{d0} = \frac{\Psi_{d0}}{I_{d0}} = \frac{\Psi_{d0co} + \Psi_{d0ew}}{I_{d0}} = L_{d0co} + L_{0ew} \tag{12}$$
$$L_{q0} = \frac{\Psi_{q0}}{I_{q0}} = \frac{\Psi_{q0co} + \Psi_{q0ew}}{I_{q0}} = L_{q0co} + L_{0ew} \tag{13}$$

Similarly, the direct component of flux linkage (the same applies for the quadrature axis) for the particular machine with distinction of the core and end-winding region is given as

$$\Psi_d = \Psi_{dco} + \Psi_{dew} = \Psi_{d0co} \frac{N_c}{a_p} \frac{l_{stk}}{l_{stk0}} + \Psi_{d0ew} \frac{N_c}{a_p} \tag{14}$$

Note that Ψ_{d0co} assumes that all conductors are connected in series with $\frac{Q_s}{3}$ turns per phase (Q_s is the number of slots), while in the particular machine the total number of turns connected in series is $\frac{Q_s}{3}\frac{N_c}{a_p}$. The ratio $\frac{l_{stk}}{l_{stk0}}$ appears because Ψ_{d0co} is the flux linkage of the referent machine with stack length l_{stk0} and the particular machine has a different stack length l_{stk}.

The direct and quadrature axis inductances are therefore

$$L_d = \frac{1}{a_p}\frac{\Psi_d}{\frac{I_d}{a_p}} = \frac{\Psi_{d0co}\frac{N_c}{a_p}\frac{l_{stk}}{l_{stk0}} + \Psi_{d0ew}\frac{N_c}{a_p}}{\frac{a_p}{N_c}I_{d0}} \tag{15}$$
$$= \frac{N_c^2}{a_p^2}\frac{l_{stk}}{l_{stk0}}L_{d0co} + \frac{N_c^2}{a_p^2}L_{d0ew} = L_{dco} + L_{ew},$$
$$L_q = \frac{N_c^2}{a_p^2}\frac{l_{stk}}{l_{stk0}}L_{q0co} + \frac{N_c^2}{a_p^2}L_{q0ew} = L_{qco} + L_{ew}. \tag{16}$$

The flux linkages in direct and quadrature axis related to permanent magnets are both equal to zero in the end region, therefore only the core components remain. If Ψ_{md0} and Ψ_{mq0} are the flux linkages due to permanent magnets for the referent machine, the particular machine will have

$$\Psi_{md} = \frac{N_c}{a_p}\frac{l_{stk}}{l_{stk0}}\Psi_{md0} = \frac{N_c}{a_p}\frac{l_{stk}}{l_{stk0}}\Psi_{md0co}, \tag{17}$$
$$\Psi_{mq} = \frac{N_c}{a_p}\frac{l_{stk}}{l_{stk0}}\Psi_{mq0} = \frac{N_c}{a_p}\frac{l_{stk}}{l_{stk0}}\Psi_{mq0co}. \tag{18}$$

The difference of inductances in direct and quadrature axis which appears in the torque equation (8) does not contain the end-winding inductance term

$$L_d - L_q = L_{dco} + L_{ew} - L_{qco} - L_{ew} = L_{dco} - L_{qco}. \tag{19}$$

The electromagnetic torque with cross-saturation effect included for the referent machine is

$$T_{em0} = \frac{3}{2}p\Big[\Psi_{md0}I_{q0} - \Psi_{mq0}I_{d0} + \left(L_{d0} - L_{q0}\right)I_{d0}I_{q0} + L_{dq0}I_{q0}^2 - L_{qd0}I_{d0}^2\Big]. \tag{20}$$

If (8) - (19) are combined with (20), the electromagnetic torque for the particular machine will be

$$T_{em} = \frac{3}{2}p\Big[\Psi_{md0}\frac{N_c}{a_p}\frac{l_{stk}}{l_{stk0}}\frac{a_p}{N_c}I_{q0} - \Psi_{mq0}\frac{N_c}{a_p}\frac{l_{stk}}{l_{stk0}}\frac{a_p}{N_c}I_{d0} + \frac{N_c^2}{a_p^2}\frac{l_{stk}}{l_{stk0}}\left(L_{d0} - L_{q0}\right)\frac{a_p^2}{N_c^2}I_{q0}I_{d0} + \frac{N_c^2}{a_p^2}\frac{l_{stk}}{l_{stk0}}L_{dq0}\frac{a_p^2}{N_c^2}\left(I_{q0}^2 - I_{d0}^2\right)\Big] = \frac{l_{stk}}{l_{stk0}}T_{em0}. \tag{21}$$

The previous equation states that the value of electromagnetic torque for a specific lamination design depends only on the stack length, but not on the number of turns per coil or the number of parallel circuits. This is very important because it means that the power and torque rating of the particular machine can be determined by simply adjusting its stack length independent of the variation of the number of turns per coil or the number of parallel circuits necessary for adjusting its voltage rating to match the voltage rating of the power converter.

The winding resistance for one phase of the referent machine is given as

$$R_0 = \rho\frac{\left(l_{stk0} + l_{ew}\right)\frac{2Q_s}{3}}{\frac{1}{2}A_{slot}f_{fill}} \tag{22}$$
$$= \rho\frac{\frac{2Q_s}{3}l_{stk0}}{\frac{1}{2}A_{slot}f_{fill}} + \rho\frac{\frac{2Q_s}{3}l_{ew}}{\frac{1}{2}A_{slot}f_{fill}} = R_{0co} + R_{0ew}.$$

where $Q_s/3$ is the number of stator slots per layer belonging to one phase of the three-phase winding, ρ is the resistivity of conductor material and l_{ew} is the length of conductor in the end region. A particular machine will have the winding resistance equal to

$$R = \frac{1}{a_p}\rho\frac{\left(l_{stk} + l_{ew}\right)\frac{2Q_s}{3a_p}N_c}{\frac{1}{2}A_{slot}f_{fill}\frac{1}{N_c}} \tag{23}$$
$$= \frac{1}{a_p}\rho\frac{\frac{2Q_s}{3a_p}N_c l_{stk}}{\frac{1}{2}A_{slot}f_{fill}\frac{1}{N_c}} + \frac{1}{a_p}\rho\frac{\frac{2Q_s}{3a_p}N_c l_{ew}}{\frac{1}{2}A_{slot}f_{fill}\frac{1}{N_c}}$$
$$= \frac{N_c^2}{a_p^2}\frac{l_{stk}}{l_{stk0}}R_{0co} + \frac{N_c^2}{a_p^2}R_{0ew} = R_{co} + R_{ew}.$$

In terms of winding resistance the proportionality with the stack length as in the case of electromagnetic torque is no longer present because the resistance in the end region is not a function of the stack length.

The direct and quadrature components of the referent machine voltage can also both be written as a sum of the components referred to the core region and end region

$$V_{q0} = \left(R_{0co}I_{q0} + \omega_0\Psi_{md0} + \omega_0 L_{d0co}I_{d0} + \omega_0 L_{dq0}I_{q0}\right) + \left(R_{0ew}I_{q0} + \omega_0 L_{0ew}I_{d0}\right) = V_{q0co} + V_{q0ew}, \tag{24}$$

$$V_{d0} = \left(R_{0co}I_{d0} - \omega_0\Psi_{mq0} - \omega_0 L_{q0co}I_{q0} - \omega_0 L_{qd0}I_{d0}\right) + \left(R_{0ew}I_{d0} - \omega_0 L_{0ew}I_{q0}\right) = V_{d0co} + V_{d0ew}, \tag{25}$$

$$V_0 = \sqrt{\left(V_{d0co} + V_{d0ew}\right)^2 + \left(V_{q0co} + V_{q0ew}\right)^2}. \tag{26}$$

In (26) V_0 represents the inverter voltage which is needed to run the referent machine at rated speed ω_0 with rated load and rated current.

Using previously derived equations it is easy to show that the voltage components related to the core region are proportional to $\frac{N_c}{a_p}\frac{l_{stk}}{l_{stk0}}$ and the end-winding components are proportional to $\frac{N_c}{a_p}$. Hence, for the particular machine one can write

$$V_q = \frac{N_c}{a_p}\frac{l_{stk}}{l_{stk0}}V_{q0co} + \frac{N_c}{a_p}V_{q0ew} \tag{27}$$
$$V_d = \frac{N_c}{a_p}\frac{l_{stk}}{l_{stk0}}V_{d0co} + \frac{N_c}{a_p}V_{d0ew} \tag{28}$$
$$V = \frac{N_c}{a_p}\frac{l_{stk}}{l_{stk0}}\sqrt{\left(V_{d0co} + \frac{l_{stk0}}{l_{stk}}V_{d0ew}\right)^2 + \left(V_{q0co} + \frac{l_{stk0}}{l_{stk}}V_{q0ew}\right)^2} \tag{29}$$

Once the stack length l_{stk} is set depending on the desired power rating of the particular machine in the series, the required voltage at rated speed (V) can be tuned to match the maximum available voltage from the power converter (V_{max}) by varying N_c and a_p. Since N_c can assume only integer values, the winding can be additionally divided into parallel circuits so that V is as close to V_{max} as possible. In reality there will always remain a certain difference between V and V_{max} in which case the actual rated speed is slightly modified compared to the rated speed of the referent machine.

The saliency ratio ξ for the referent and particular machine is given as

$$\xi_0 = \frac{L_{q0}}{L_{d0}} = \frac{L_{q0co} + L_{0ew}}{L_{d0co} + L_{0ew}} \tag{30}$$

$$\xi = \frac{L_q}{L_d} = \frac{L_{qco} + L_{ew}}{L_{dco} + L_{ew}} = \frac{\frac{N_c^2}{a_p^2}\frac{l_{stk}}{l_{stk0}} L_{q0co} + \frac{N_c^2}{a_p^2} L_{0ew}}{\frac{N_c^2}{a_p^2}\frac{l_{stk}}{l_{stk0}} L_{d0co} + \frac{N_c^2}{a_p^2} L_{0ew}} \tag{31}$$

$$= \frac{L_{q0co} + \frac{l_{stk0}}{l_{stk}} L_{0ew}}{L_{d0co} + \frac{l_{stk0}}{l_{stk}} L_{0ew}}$$

The normalized characteristic current $I_{c,pu}$ for the referent and particular machine is given as

$$I_{c0,pu} = \frac{\Psi_{md0}}{L_{d0} I_0} = \frac{\Psi_{md0}}{(L_{d0co} + L_{0ew}) I_0} \tag{32}$$

$$I_{c,pu} = \frac{\Psi_{md}}{L_d I} = \frac{\Psi_{md0} \frac{N_c}{a_p} \frac{l_{stk}}{l_{stk0}}}{\left(\frac{N_c^2}{a_p^2}\frac{l_{stk}}{l_{stk0}} L_{d0co} + \frac{N_c^2}{a_p^2} L_{d0ew}\right) \frac{a_p}{N_c} I_0} \tag{33}$$

$$= \frac{\Psi_{md0}}{\left(L_{d0co} + \frac{l_{stk0}}{l_{stk}} L_{d0ew}\right) I_0}$$

If one considers the fact that in an actual machine the end-winding leakage inductance is at least one or two orders of magnitude smaller than inductances in direct or quadrature axis of the core region, then the saliency ratio or the normalized characteristic current of the referent and the particular machine designs will be very close. The exception to this rule are particular machine designs with stack lengths significantly smaller than the stack length of the referent machine, because in that case the share of the end-winding leakage inductance increases and might result in non-negligible reduction of the saliency ratio or the characteristic current. This is why it is useful to select l_{stk0} to be close to the stack lengths of the particular designs in the series. The problem is the fact that for a new design it is not known in advance what will be the torque developed per unit stack length so that l_{stk0} can be chosen optimally. In that case some initial rule of thumb estimate can be made and after obtaining the optimal lamination design for the referent machine the actual stack lengths of the particular designs in the series can be determined. If these stack lengths are not significantly different from l_{stk0} so that variation of parameters due to influence of the end-winding region is negligible, then the series can be formed based on the current referent design. If this is not the case, the stack length l_{stk0} can be corrected and a new referent design can be found.

The copper losses are given as

$$P_{Cu0} = 3 I_0^2 R_0 = 3 I_0^2 \left(R_{0co} + R_{0ew}\right) \tag{34}$$

$$P_{Cu} = 3 I^2 R = 3 \frac{a_p^2}{N_c^2} I_0^2 \left(\frac{N_c^2}{a_p^2}\frac{l_{stk}}{l_{stk0}} R_{0co} + \frac{N_c^2}{a_p^2} R_{0ew}\right) \tag{35}$$

$$= 3 I_0^2 \left(\frac{l_{stk}}{l_{stk0}} R_{0co} + R_{0ew}\right)$$

The copper losses in the core region will change proportionally to the change of the stack length of the particular machine relative to the stack length of the referent machine. As expected, the copper losses in the end-winding region will remain the same if the conductor length l_{ew} is the same for all designs. The variation of N_c or a_p does not affect the copper losses as long as the current density in the winding remains the same.

The core losses can be estimated using the standard Steinmetz formula

$$P_{c0} = \int_{A_c} \left(k_h B^\alpha f + k_e B^2 f^2\right) l_{stk0} f_{stk} \mathrm{d}A_c \tag{36}$$

$$P_c = \int_{A_c} \left(k_h B^\alpha f + k_e B^2 f^2\right) l_{stk} f_{stk} \mathrm{d}A_c = \frac{l_{stk}}{l_{stk0}} P_{c0} \tag{37}$$

where k_h and k_e are the coefficients of hysteresis and eddy current losses of the steel sheets, B is the flux density in the core, f_{stk} is the stack fill factor, f is the frequency of the field and A_c is the core area. The iron losses of the particular design in the series will be scaled in the ratio of its stack length to the stack length of the referent machine.

The input active power can be written as

$$\begin{aligned} P_{in} &= 3(V_d I_d + V_q I_q) = 3 V I cos\varphi \\ &= 3\sqrt{\left(V_q^2 + V_d^2\right)\left(I_q^2 + I_d^2\right)} cos\varphi \end{aligned} \tag{38}$$

The power factor is equal to the ratio of input active and apparent power

$$cos\varphi = \frac{P_{in}}{S_{in}} = \frac{V_d I_d + V_q I_q}{\sqrt{\left(V_q^2 + V_d^2\right)\left(I_q^2 + I_d^2\right)}} \tag{39}$$

Combining (11), (27) and (28) with (39) yields

$$cos\varphi_0 = \frac{\left(V_{d0co} + V_{d0ew}\right) I_{d0} + \left(V_{q0co} + V_{q0ew}\right) I_{q0}}{\sqrt{\left[\left(V_{d0co} + V_{d0ew}\right)^2 + \left(V_{q0co} + V_{q0ew}\right)^2\right]} I_0} \tag{40}$$

$$cos\varphi = \frac{\left(V_{d0co} + \frac{l_{stk0}}{l_{stk}} V_{d0ew}\right) I_{d0} + \left(V_{q0co} + \frac{l_{stk0}}{l_{stk}} V_{q0ew}\right) I_{q0}}{\sqrt{\left[\left(V_{d0co} + \frac{l_{stk0}}{l_{stk}} V_{d0ew}\right)^2 + \left(V_{q0co} + \frac{l_{stk0}}{l_{stk}} V_{q0ew}\right)^2\right]} I_0} \tag{41}$$

for the referent and particular machine design. In terms of variation of the power factor the same comments made for the saliency ratio and the normalized characteristic current regarding the influence of the the end-winding region and the stack lengths of the referent and particular designs are valid in this case as well.

The torque density is given as

$$T_{density0} = \frac{T_{em0}}{V_0} = \frac{T_{em0}}{\frac{D_0^2}{4}\pi l_{stk0}} \tag{42}$$

$$T_{density} = \frac{T_{em}}{V} = \frac{\frac{l_{stk}}{l_{stk0}} T_{em0}}{\frac{l_{stk}}{l_{stk0}} V_0} = T_{density0} \tag{43}$$

The efficiency for the motoring regime is calculated as the ratio of output mechanical power and input electrical power

$$\eta = \frac{P_{out}}{P_{in}} = \frac{T_{em}\omega_0 - P_c - P_{f,w}}{3 V I cos\varphi} = \frac{T_m \omega_0}{3(V_d I_d + V_q I_q)} \tag{44}$$

where T_m is the actual mechanical torque on the rotor shaft. If it is assumed that the friction and windage losses ($P_{f,w}$) are proportional to the stack length and using previously derived equations, it is easy to show that the efficiency of the referent and particular machine will be

$$\eta_0 = \frac{T_{em0}\omega_0 - P_{c0} - P_{fr,w0}}{3\left[\left(V_{d0co} + V_{d0ew}\right) I_{d0} + \left(V_{q0co} + V_{q0ew}\right) I_{q0}\right]} \tag{45}$$

$$\eta = \frac{T_{em0}\omega_0 - P_{c0} - P_{f,w0}}{3\left[\left(V_{d0co} + \frac{l_{stk0}}{l_{stk}} V_{d0ew}\right) I_{d0} + \left(V_{q0co} + \frac{l_{stk0}}{l_{stk}} V_{q0ew}\right) I_{q0}\right]} \quad (46)$$

With the increase of the power rating the stack length of the particular machine also increases. For instance, if l_{stk0} is chosen to be the average value of minimum and maximum stack lengths of the particular designs in the series, then as the power rating increases above the rating of the referent design the denominator of (46) reduces leading to the increase of efficiency. For power ratings dropping below the power rating of the referent machine the opposite is valid. This is expected since efficiency usually increases with the increase of the power rating of the machine for a certain type of design.

III. Example of the Optimized IPM Motor Series

In order to demonstrate the correctness of the design principles for the IPM motor series derived in the previous section, an optimized design of a referent machine has been made using Differential Evolution [7] optimization algorithm. The 2D magnetostatic FE simulations have been used in the optimisation procedure for calculation of the motor torque, flux linkages, inductances, losses etc.

Five particular designs with different power ratings have been derived from the optimal referent design. The basic foundation for the design is the IEC frame size 160 denoting the distance between the horizontal surface and the centerline of the shaft of a foot mounted frame (IM B3) [8]. This frame size defines the constant outer diameter of the stator core for all particular design in the series. The specific requirements for the series are defined in Table I.

The shaft diameter has been set for the maximum power rating in the series. For lower power ratings smaller shaft diameters can be used due to reduced shaft torque. In this particular case the integral slot winding has been selected to reduce the optimization time since in that case only one pole pitch can be modeled. However, in order to obtain a design with lower torque ripple it is advisable to use the fractional slot winding. For instance, the slot/pole combination 27/6 can be used as shown in [9] because designs with nine slots per pole pair can be optimized for other machine performance criteria, while keeping the torque ripple low. In addition, the location and width of the rotor yoke channel between the inner and outer layers of the rotor cavities in a two-layer rotor can be adjusted to reduce the rotor core [10] or the stator teeth [11] eddy current losses in the flux weakening operation at high speed.

For the optimized design of the IPM motor series presented in this paper the emphasis has been on the maximization of the developed rated torque at rated speed (T_{r0}) of the referent machine design and the extension of the constant power region up to desired maximum speed. The optimization problem has been defined in the following manner:

Maximize the cost function

$$F = -T_{r0} \quad (47)$$

subject to inequality constraints

1) Power output at maximum speed: $P_{out\omega_{max}} \geq P_{outr}$,
2) Flux density in the stator core tooth: $B_{ts} \leq 1.8$ T,
3) Flux density in the stator yoke: $B_{ys} \leq 1.3$ T,
4) Linear current density along stator bore: $K \leq 40000$ Arms/m.
5) Minimum allowed flux density in the permanent magnet at transient peak current during symmetrical short circuit: $B_{PMmin} \geq B_{knee}$@100°C+0.2 T,

The negative value of the rated torque in the cost function has been defined because the default for the optimization algorithm is to minimize the cost function. The inequality constraints have been handled within the DE code using the approach by Lampinen [7]. In order to ensure the resistance to demagnetization, the minimum flux density in the magnets is calculated using FEM for the case when the armature winding field is applied in the direction of the negative direct axis using the transient peak current during symmetrical short circuit in the regenerative operation at rated speed, which is identified in [12] as the worst case short-circuit current. The minimum flux density must be greater than the flux density at the knee point of the PM material at 100 degrees Celsius with 0.2 T added as a safety factor.

The design variables are listed in Table II together with their limits. All geometric variables have been normalized. The discrete variables have been included in the basic DE algorithm using the approach proposed by Lampinen and Zelinka [13]. The permanent magnet materials listed in Table III are selected from the manufacturer's catalogue. The choice has been reduced to materials suitable for continuous operation at temperatures up to 180°C or higher. The span of the cavities relative to the pole pitch has been adjusted to discrete values for minimizing the fundamental component of the cogging torque as defined in [14]. The magnets of rectangular shape fill only the horizontal cavities, while the slanted cavities are filled with air.

The stator core losses have been calculated using (36). The rotor core losses have been neglected during optimization. No detailed analysis has been carried out to determine accurate expressions for friction and windage losses. Instead, simple equations given by Gieras [15] have been used to estimate these losses. According to [15], the friction losses are given by

$$P_{fr} = k_{fb} m_r n_{rm} 10^{-3} \quad (48)$$

where $k_{fb} = 1.5$ is an empirical coefficient ranging from 1 to 3, m_r is the mass of the rotor and n_{rm} is the rotor mechanical speed in rpm. The windage losses for the speeds below 6000 rpm can be approximated using

$$P_w = 2 D_{ro}^3 l_{stk} n_{rm}^3 10^{-6} \quad (49)$$

where D_{ro} is the outer diameter of the rotor and l_{stk} is the stack length.

The result of the optimization is the referent motor which satisfies all the imposed constraints and yields the highest rated torque of 218.4 Nm at 1800 rpm within the defined core volume. The cross section of one pole pitch of the referent design with flux lines at rated operating point is shown in Fig. 1. By adjusting the stack length to obtain the desired power output a series of designs is obtained whose main parameters have been listed in Table IV. For calculation of inductances and permanent-magnet flux linkage at rated speed and torque and for solving the voltage equation the values of permeability in the nodes of the finite-element mesh have been frozen and the parameters have been

TABLE IV
FINAL RESULTS FOR THE DESIGN OF THE IPM MOTOR SERIES

	Ref. design	*Particular designs*				
Targeted output power at 1800 rpm, kW	maximized	15	30	45	75	110
Number of turns per coil	1	56	28	19	11	8
Number of parallel circuits	1	6	6	6	6	6
Stack length, mm	300	110	222	328	547	802
Corner speed, rpm	1800	1799	1804	1806	1878	1762
Output power at corner speed, kW	41.159	15.084	30.527	45.158	78.287	107.72
Output power at targeted corner speed (1800 rpm), kW	41.159	15.091	30.467	45.022	75.478	109.72
Output power at maximum speed (5400 rpm), kW	41.416	15.637	30.943	45.424	79.408	106.22
Saliency ratio	2.366	2.335	2.360	2.368	2.375	2.378
Normalized characteristic current	1.226	1.198	1.22	1.227	1.234	1.237
cosφ	0.886	0.882	0.885	0.886	0.887	0.887
Efficiency at corner speed	0.9708	0.9604	0.9687	0.9714	0.9743	0.9743

TABLE I
SPECIFIC DESIGN REQUIREMENTS FOR THE IPM MOTOR SERIES

Parameter	*Symbol*	*Value*	*Unit*
BASIC REQUIREMENTS			
Rated output power	P_{outr}	15, 30, 45, 75, 110	kW
Rated line-to-line voltage (rms)	V_r	400	V
Rated speed	n_r	1800	rpm
Maximum speed for constant power operation	n_{max}	5400	rpm
PRESET CONSTANTS			
Stator outer diameter	D_o	240	mm
Rotor inner (shaft) diameter	D_{sh}	85	mm
Number of pole pairs	p	3	–
Number of slots	Q_s	36	–
Air-gap length	g	0.7	mm
Referent design stack length	l_{stk0}	300	mm
Slot fill factor	f_{fill}	0.4	–
Current density	J_0	4.5	A/mm^2

TABLE II
VARIABLES USED IN THE OPTIMIZED DESIGN OF THE IPM MOTOR SERIES

Variable	*Variable type*	*Limits*
Ratio of stator inner diameter to outer diameter	continuous	$0.45 \leq \frac{D_{in}}{D_o} \leq 0.75$
Ratio of stator yoke thickness to difference between stator outer and inner radius	continuous	$0.2 \leq \frac{d_{ys}}{R_o - R_{in}} \leq 0.6$
Ratio of stator tooth width to slot pitch at D_{in}	continuous	$0.3 \leq \frac{b_{ts}}{\tau_s} \leq 0.7$
Ratio of total cavity to total rotor core depth	continuous	$0.05 \leq \lambda_m \leq 0.5$
Relative rotor core depth for the outermost rotor core section	continuous	$0.2 \leq \lambda_{md1} \leq 0.6$
Relative rotor core depth for the rotor core section between the cavities	continuous	$0.1 \leq \lambda_{md2} \leq 0.4$
Relative angle of the slanted cavities	continuous	$0.5 \leq \frac{\beta}{\frac{\pi}{2}\left(1-\frac{1}{p}\right)} \leq 1$
Span of the inner cavity relative to the pole pitch	discrete	$1 - k\frac{2p}{\mathrm{lcm}(Q_s,2p)} + 0.02, k = 1, 2$
Permanent magnet properties	discrete	Tabular input

TABLE III
PROPERTIES OF THE SELECTED PERMANENT MAGNET MATERIALS AT 100°C

Material type	*Remanent flux density,* B_r[T]	*Relative permeability,* μ_r	*Flux density at the knee point,* B_{knee}[T]
VACODYM 872 TP	1.155	1.0308	-0.64
VACODYM 677 TP	1.100	1.026	-0.7
VACODYM 863 AP	1.144	1.041	-0.4
VACODYM 669 AP	1.100	1.043	-0.5

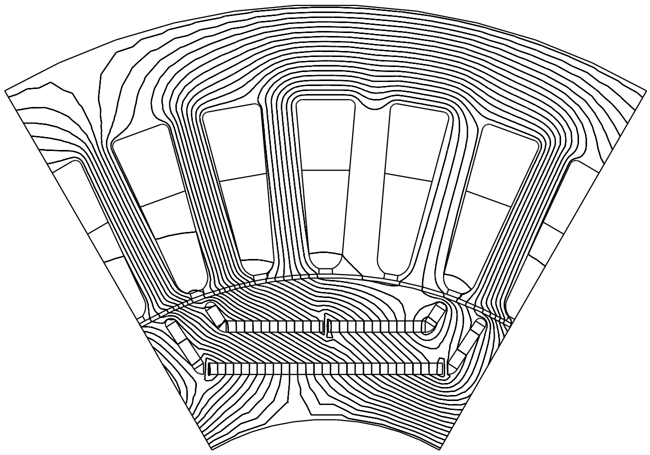

Fig. 1. Cross section of the optimized referent machine design with flux lines at rated operating point

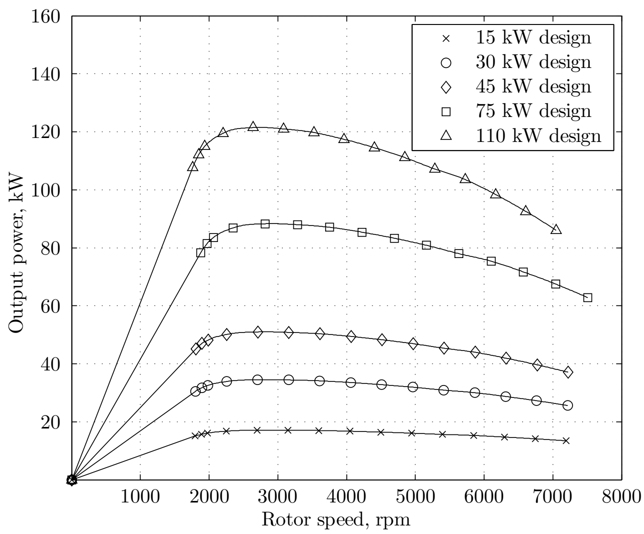

Fig. 2. Calculated power output vs speed curves for all designs in the series

calculated in a sequence of linear simulations with the same nodal values of permeability. The same procedure is used for all calculated operating points. Fig. 2 shows the mechanical output power for all designs in the series. The results in Table IV are in accordance with the conclusions made in Section II. For the first three particular designs it was possible to adjust the stack length to achieve the desired power outputs at corner speeds very close to the desired value of 1800 rpm. The last two designs rated 75 kW and 110 kW were somewhat problematic because the desired power outputs were obtainable only at corner speeds above (75 kW) and below (110 kW) 1800 rpm. In the case of the 75 kW design for stack lengths shorter than the value in the table the corner speed increases above the value in the table, while the output power decreases below the desired value at 1800 rpm. For higher stack lengths the corner speed gets closer to 1800 rpm, but the output power at 1800 rpm becomes higher than desired resulting in an overrated motor design.

In the case of the 110 kW design for stack lengths shorter than the value in the table the corner speed increases towards 1800 rpm, but the desired power output cannot be reached at that desired speed. For higher stack lengths the corner speed further decreases below the value in the table, but at the same time the output power increases above 110 kW.

In these two cases the problem is that for each power rating and the corresponding stack length there exists an optimal ratio $\frac{N_c}{a_p}$ which yields the required power output at the required corner speed. However, since N_c and a_p can assume only integer values, there is only a finite number of combinations for their ratio within the allowed maximum a_p, which is limited to six in this particular case. The limit is imposed because as a_p increases the N_c increases as well, while the current in each parallel circuit decreases resulting in a high number of strands with small diameter and complicated connections of parallel circuits. This complicates the winding assembly and increases its manufacturing cost. The higher is the difference between the required and obtainable $\frac{N_c}{a_p}$ the more difficult it is to adjust the power output and corner speed at the same time. In that case more favorable designs are those with corner speed higher than desired because those designs will be able to ensure the constant power operation up to desired maximum speed. If the actual corner speed is lower than desired, it is still possible to reach the required power output at the desired corner speed, but at that speed the machine is already in the flux weakening operation and hence its constant power region will most likely end at the speed below the desired maximum speed. This is the case with the 110 kW design in our example.

The selection of the rotor configuration, flux barriers and winding configuration for minimization of the torque ripple, the rotor losses or for improvement of some other feature have not been the primary focus of this paper although such goals can be easily introduced into presented optimization procedure. The use of rare earth magnets is also not mandatory here. The same approach for designing the IPM motor series can be used for motors with ferrite magnets and a different stator or rotor configuration. The analytical formulae derived in this paper are invariable of the rotor configuration because they are based on the phasor diagram with variables such as flux linkages, currents, voltages and inductances that can be calculated for any rotor design.

IV. Conclusion

A general approach to optimized design of a series of interior permanent magnet motors with the same lamination cross section has been presented. A concept of a referent design has been introduced which can be optimized according to a certain criterion and from which all the particular designs in the series can be derived. Therefore it is possible to tune all the particular designs very close to the desired power ratings and close to the desired corner speed while maintaining the constant power operation up to the same desired maximum speed with the same maximum available voltage from the power converter. The perfect tuning is not always possible due to limited number of combinations of the number of turns per coil and the number of parallel circuits, although it can be achieved if the desired power ratings of the motors in the series are slightly adjusted. The contribution of this paper is a definition of the basic approach for designing a series of IPM motors by showing that variation of the stack length, the number of turns per coil and the number of parallel circuits in order to obtain the desired power rating does not affect the parameters that determine important machine characteristics. This is feasible if certain general assumptions provided in the paper are followed.

References

[1] L. Alberti, N. Bianchi, and S. Bolognani, “Lamination Design of a Set of Induction Motors,” *Journal of Electrical Engineering: Theory and Application*, vol. 1, pp. 18–23, 2010.

[2] E. Lovelace, T. Jahns, and J. Lang, “Impact of saturation and inverter cost on interior PM synchronous machine drive optimization,” *IEEE Transactions on Industry Applications*, vol. 36, no. 3, pp. 723–729, 2000.

[3] W. Soong, N. Ertugrul, E. Lovelace, and T. Jahns, “Investigation of interior permanent magnet offset-coupled automotive integrated starter/alternator,” in *Conference Record of the 2001 IEEE Industry Applications Conference. 36th IAS Annual Meeting (Cat. No.01CH37248)*, vol. 1. IEEE, 2001, pp. 429–436.

[4] E. Lovelace, T. Jahns, T. Keim, and J. Lang, “Mechanical Design Considerations for Conventionally Laminated, High-Speed, Interior PM Synchronous Machine Rotors,” *IEEE Transactions on Industry Applications*, vol. 40, no. 3, pp. 806–812, May 2004.

[5] N. Bianchi, S. Bolognani, D. Bon, and M. Dai Pre, “Rotor flux-barrier design for torque ripple reduction in synchronous reluctance and pm-assisted synchronous reluctance motors,” *Industry Applications, IEEE Transactions on*, vol. 45, no. 3, pp. 921 –928, may-june 2009.

[6] R. Schiferl and T. Lipo, “Power capability of salient pole permanent magnet synchronous motors in variable speed drive applications,” *IEEE Transactions on Industry Applications*, vol. 26, no. 1, pp. 115–123, 1990.

[7] J. Lampinen, “Multi-Constrained Nonlinear Optimization by the Differential Evolution Algorithm,” in *6th On-line World Conference on Soft Computing in Industrial Applications (WSC6)*, 2001, pp. 1–19.

[8] *INTERNATIONAL STANDARD IEC60034-7, Rotating electrical machines Part 7: Classification of types of construction, mounting arrangements and terminal box position (IM Code) 2.1.* (IEC), International Electrotechnical Commission.

[9] S. Han, T. Jahns, W. Soong, M. Guven, and M. Illindala, “Torque Ripple Reduction in Interior Permanent Magnet Synchronous Machines Using Stators With Odd Number of Slots Per Pole Pair,” *IEEE Transactions on Energy Conversion*, vol. 25, no. 1, pp. 118–127, Mar. 2010.

[10] S. Han, T. Jahns, and Z. Zhu, “Analysis of rotor core eddy-current losses in interior permanent-magnet synchronous machines,” *IEEE Transactions on Industry Applications*, vol. 46, no. 1, pp. 196–205, 2010.

[11] S. Han, W. Soong, T. Jahns, M. Guven, and M. Illindala, “Reducing harmonic eddy-current losses in the stator teeth of interior permanent magnet synchronous machines during flux weakening,” *IEEE Transactions on Energy Conversion*, vol. 25, no. 2, pp. 441–449, 2010.

[12] M. Meyer and J. Bocker, “Transient peak currents in permanent magnet synchronous motors for symmetrical short circuits,” in *International Symposium on Power Electronics, Electrical Drives, Automation and Motion, 2006. SPEEDAM.* IEEE, 2006, pp. 404–409.

[13] J. Lampinen and I. Zelinka, “Mixed Integer-Discrete-Continuous Optimization By Differential Evolution - Part 1: the optimization method,” in *5th International Mendel Conference on Soft Computing*, 1999, pp. 71–76.

[14] Z. Zhu and D. Howe, “Influence of design parameters on cogging torque in permanent magnet machines,” *IEEE Transactions on Energy Conversion*, vol. 15, no. 4, pp. 407–412, 2000.

[15] J. Gieras and M. Wing, *Permanent Magnet Motor Technology*. New York, Basel: Marcel Dekker, 2002.

Damir Žarko was born in Zagreb, Croatia. He received the Dipl. Eng. and M.Sc. degrees in electrical engineering from the University of Zagreb in 1995 and 1999 respectively and the Ph.D. degree from the University of Wisconsin-Madison in 2004. Currently he is an Assistant Professor at the Department of Electrical Machines Drives and Automation, Faculty of Electrical Engineering and Computing, University of Zagreb, Croatia where his research activities are related to design, modelling, analysis and optimization of electrical machines.

Stjepan Stipetić was born in Ogulin, Croatia. He received Dipl. Eng. degree in electrical engineering from the University of Zagreb, Croatia in 2008. Currently he is a Ph.D. student working as a junior researcher at the Department of Electric Machines, Drives and Automation, Faculty of Electrical Engineering and Computing, University of Zagreb. His areas of interest include design, modelling, analysis and optimization of electrical machines.